

AD P001035

STRUCTURAL ANALYSIS OF A MINE WITH TWO VISCOELASTIC EXPLOSIVE FILLS

Aaron D. Gupta
Mechanical Engineer

U.S. Army Ballistic Research Laboratory
U.S. Army Armament Research and Development Command
Aberdeen Proving Ground, Maryland 21005

ABSTRACT. The structural response of a Soviet TM-46 land mine with two viscoelastic explosive fills subjected to an externally applied pressure wave has been analyzed with the ADINA finite element code. The main charge consists of 5.72 kg TNT while the booster charge in the fuze contains .04 kg Tetryl in the fuze well. The finite element model of the mine uses the axisymmetric two-dimensional mesh configuration with a rigid base support boundary condition. Both implicit and explicit time integration schemes have been used for this analysis.

The viscoelastic explosive filler materials exhibit marked nonlinear behavior. It was therefore decided that the tension cut-off curve description material models were the appropriate models to use. Relationships between the volume strains and the bulk moduli were obtained from the Mie-Grüneisen equations of state. These models include failure criteria which allow tension cut-off planes to form in a direction normal to the principal tensile stress whenever the strain initially exceeds 0.1% in tension. The materials for the steel casing were modeled with bilinear stress-strain curves, von Mises yield condition, and kinematic hardening rule. Trapped air inside the mine body was modeled as an assembly of inviscid linear compressible fluid elements.

The finite element model was initially verified for mode shapes at a few low order eigenfrequencies and a failure criterion for the casing was incorporated based on a comparison of the value of the three-dimensional second invariant of plastic strain with that of the one-dimensional value obtained from the tensile tests. Solution of the problem in terms of stresses and displacements out to .75 ms of real time indicates high stress concentration and large displacements of the top cover plate in the stepped region and minimal response of the interior structure until the cover plate is in contact with the intermediate partition of the mine body.

1. INTRODUCTION. This paper describes the response of the Soviet TM-46 Antitank mine with a unique double walled construction of the top pressure plate designed to resist a transient blast load. The rationale for this analysis is the need to develop a remote, expeditious means of clearing a path through an enemy mine field. A method of imparting a relatively large transient pressure and impulse to the surface of the earth by means of explosives is under development. The current study is a part of a general investigation to determine the extent of structural damage sustained by the mine body from a given level of blast wave amplitude and shape. The principal kill mechanism is to be a serious distortion or rupture of the mine casing rather than fuze initiation or removal of pressure plate since the damage mechanisms could be easily changed from a particular type of mine to another and a surekill could not be ensured based on a particular mode of actuation.

The mine investigated represents a typical Soviet antitank mine, which consists basically of a round thin metal body filled with an explosive. The unique feature of this mine is a double walled construction of the top wall resulting from joining of the top pressure plate with the intermediate wall along the circular edge through a crimped joint which tends to increase the blast resistance behavior of the mine. The other distinctive feature is the fuze mechanism. However a variety of radically different fuzes, different both in mechanical designs and method of activation could be substituted for the currently used ball-spring mechanism. Therefore the numerical model in the present study does not include a model of the fuze.

The paper has four major areas as follows: (a) problem definition, (b) determination of material properties and selection of failure criteria of the casing as well as numerical characterization of the viscoelastic explosive fills, (c) finite element model description and calculations, and (d) dynamic response prediction of the structural assembly.

2. PROBLEM DEFINITION.

A. Antitank Mine Description. The TM-46 land mine has a cylindrical steel body with a primary fuze well in the center of the top and one at the bottom, presumably for antilift or booby trapping purposes. In addition, it has a secondary fuze well in the sidewall underneath the carrying handle. A sectional drawing of the mine is shown in Figure 1. The mine has a nominal diameter of 29.7 cm, height of 7.3 cm and weighs 8.7 kg with a main charge of 5.7 kg TNT.

The mine body is made of three pieces of sheet steel which are joined at the upper periphery by a 360° crimp. The top cover of the mine body is only 0.635 mm thick and has three steps. This cover connects to a central circular plate formed by spot-welding of a thick plate to the thin cover section. The intermediate wall is formed from 0.94 mm thick steel sheet to which a hollow cylindrical piece 0.56 mm thick is attached to form the centrally located top fuze well. The fuze well contains a 40 g tetryl booster charge for fuze activation.

The lower part of the mine body is formed by a deep drawing operation which results in very inhomogenous material properties. The central cavity in the main body of the mine is filled with a charge of 5.7 kg TNT explosive. The cavity between the top and intermediate walls is unfilled. However compression of air in this region can contribute to alteration of the response behavior of the mine and subsequent uncrimping of the joint.

The normal method of activation of the fuze is by means of force applied to the pressure cap depressing the fuze and releasing the striker to strike the booster charge in the fuze well. This activates the tetryl booster which in turn detonates the primary TNT charge. The secondary fuze well on the TM-46 mine gives it anti-disturbance capability.

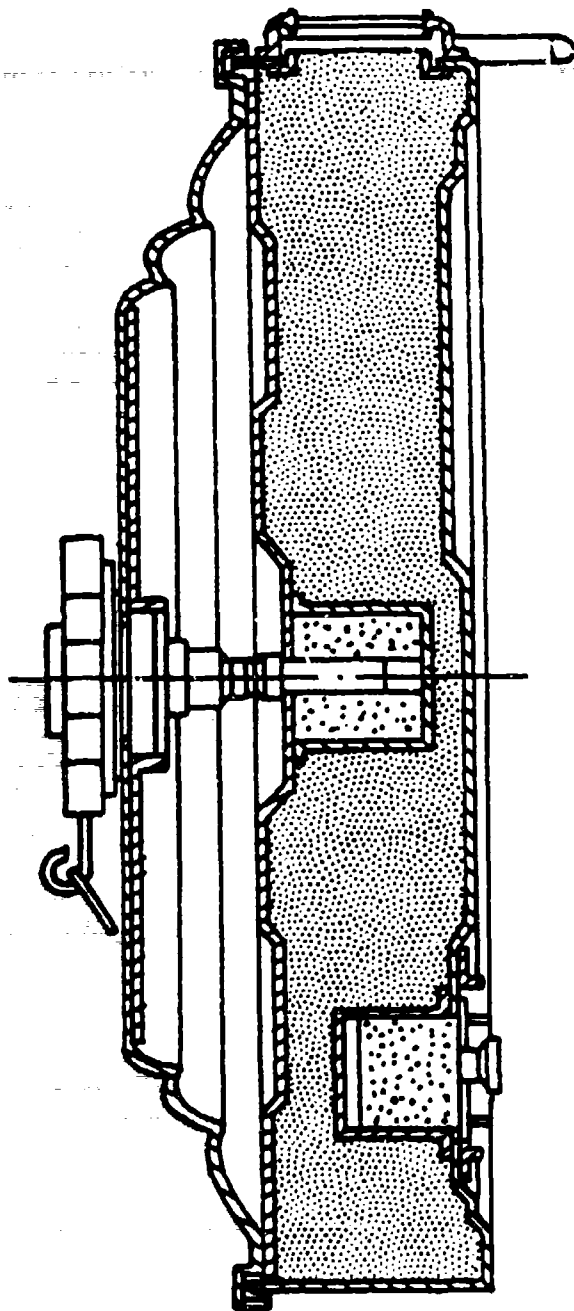


Figure 1. Soviet Anti-tank Mine Model TM-46

B. Guidelines for the Numerical Model. In keeping with the objective of identifying a general failure mechanism independent of some specific design feature, all fuzes and springs were omitted from the finite element model of the mine. This was done in accordance with the previously stated guideline of not identifying failure of the fuze components. The model considered for this study does not include secondary fuzes and filling holes. However the secondary tetryl booster charge is included to facilitate assessment of the influence of trapped air in the unfilled space below the top wall on structural response of the mine.

The auxiliary fuze wells were not considered in the current investigation since they increase susceptibility of the mine to damage due to stress concentration near the junction between the body and the fuze. Thus, the simplified model is conservative in terms of blast load requirements for mine deactivation. Also, inclusion of these unsymmetrically loaded structures would require the use of a three-dimensional (3-D) finite element model resulting in significant increase in computing time and costs. The dimples at the base of the mine were eliminated for the same reasons. Because of these simplifications the 2-D axisymmetric model was cost-effective and conservative for dynamic response evaluation.

C. Base Support and Surface Loading. During field emplacement, the mines may be placed on the surface and covered with grass or other materials for concealment. In other cases, the mine may be shallow buried. In both cases, the mine will experience transient pressure loading on the top surface due to detonation of a countermine explosive in the vicinity. It is expected that typical field boundary support conditions would be bracketed by two extreme situations. In one case, the mine could be simulated as being buried in soil up to its top surface while the base is supported on nonlinear springs as described in Reference 1. The other support condition allows the mine to be supported on a rigid roller base which closely models the experimental conditions described in Reference 2. In the current study only the second support condition was simulated in the numerical model but inclusion of the soil medium implicitly through nonlinear spring node-tie boundary elements or explicitly through dynamic property characterization of the soil could be made without significant change in the basic model. A roller support condition was used allowing lateral, but no vertical, motion. In this rigid support condition, the input shock load is applied to the top and sides of the mine.

For structural loading the pressure pulse used in this paper simulated peak pressure and impulse measured from experiments conducted with mine clearance types of explosives in Reference 2. The peak pressure was 13.8 MPa and the impulse delivered was 6.5 kPa-sec. A decaying exponential function was fitted to these parameters resulting in the following equation

$$P(t) = 13.76e^{-2117t} \quad (1)$$

A curve of this function varying in time is shown in Figure 2.

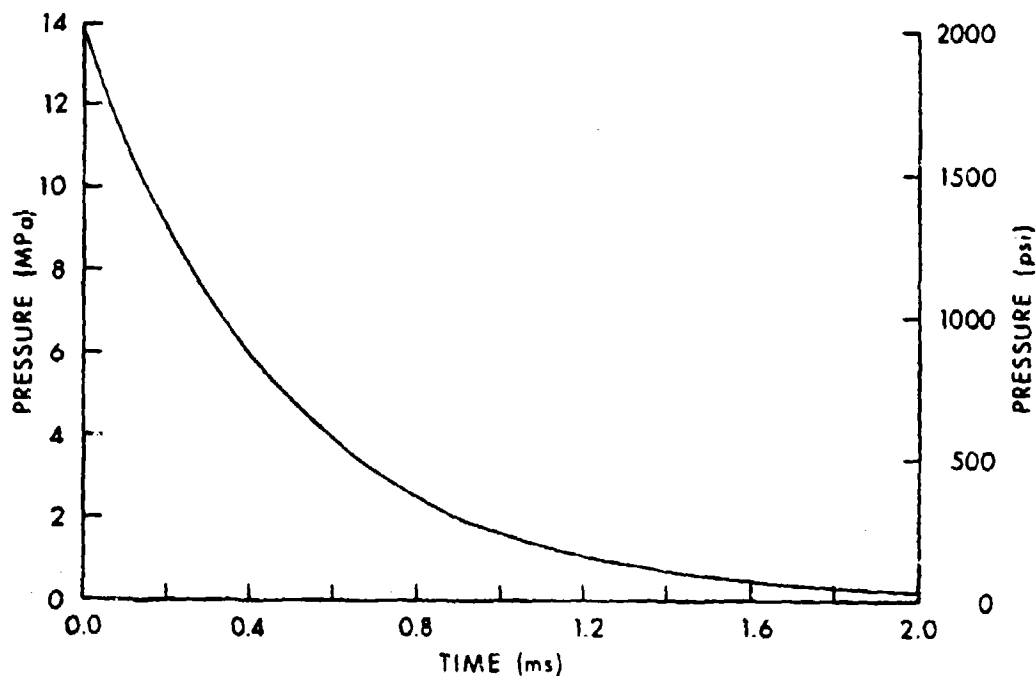
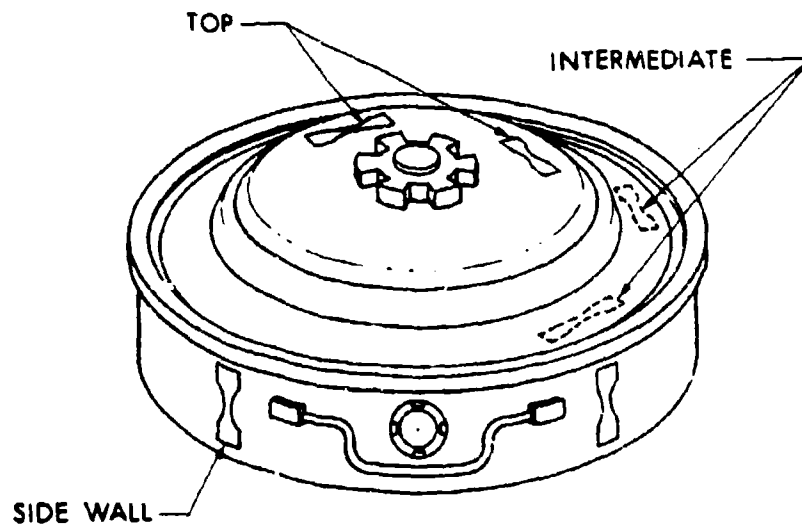


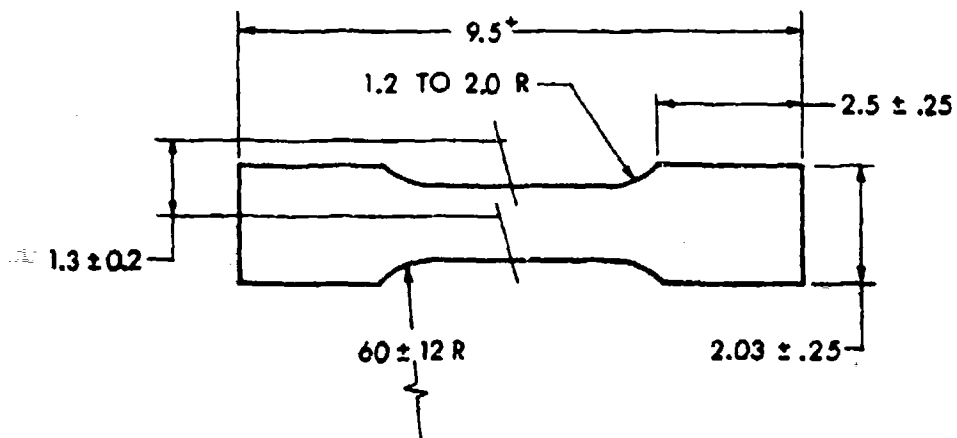
Figure 2. Shock Loading in Antitank Mines

3. MATERIAL PROPERTIES CHARACTERIZATION AND FAILURE CRITERIA. Material properties were required for the steel jackets, the explosive filler materials and the trapped air before numerical simulation could be carried out. Mechanical properties were measured for the steel jackets by employing uniaxial tensile tests. The high pressure equation of state data for explosives were obtained from available publications. Failure criteria used for the steel jackets and the filler materials were similar to the formulations in Reference 3.

A. Steel Casing. The TM-46 jacket is made of a low carbon soft magnetic steel equivalent to mild steel. The lower part of the casing was deep drawn, but it retained an equiaxed grain microstructure with isotropic properties. Two tensile specimens were cut from each of the significant surfaces of the mine body. Locations of these specimens are shown in Figure 3(a). The specimens were machined with a large radius on the test section as shown in Figure 3(b). An extensometer and a biaxial strain gage were attached at the location of the minimum width and the specimens were tested in an Instron Testing Machine at a relatively slow rate of strain. Typical quasi-static stress-strain curves for the Soviet mine body are shown in Figure 4. Evidence of work hardening and residual stress was significant in the casing material due to the forming operation and operating field conditions.



(a) LOCATION OF SPECIMENS, TM-46 MINE



(b) PREPARATION OF SPECIMEN DIMENSIONS (cm)

Figure 3. Details of Tensile Specimen Sampling and Preparation

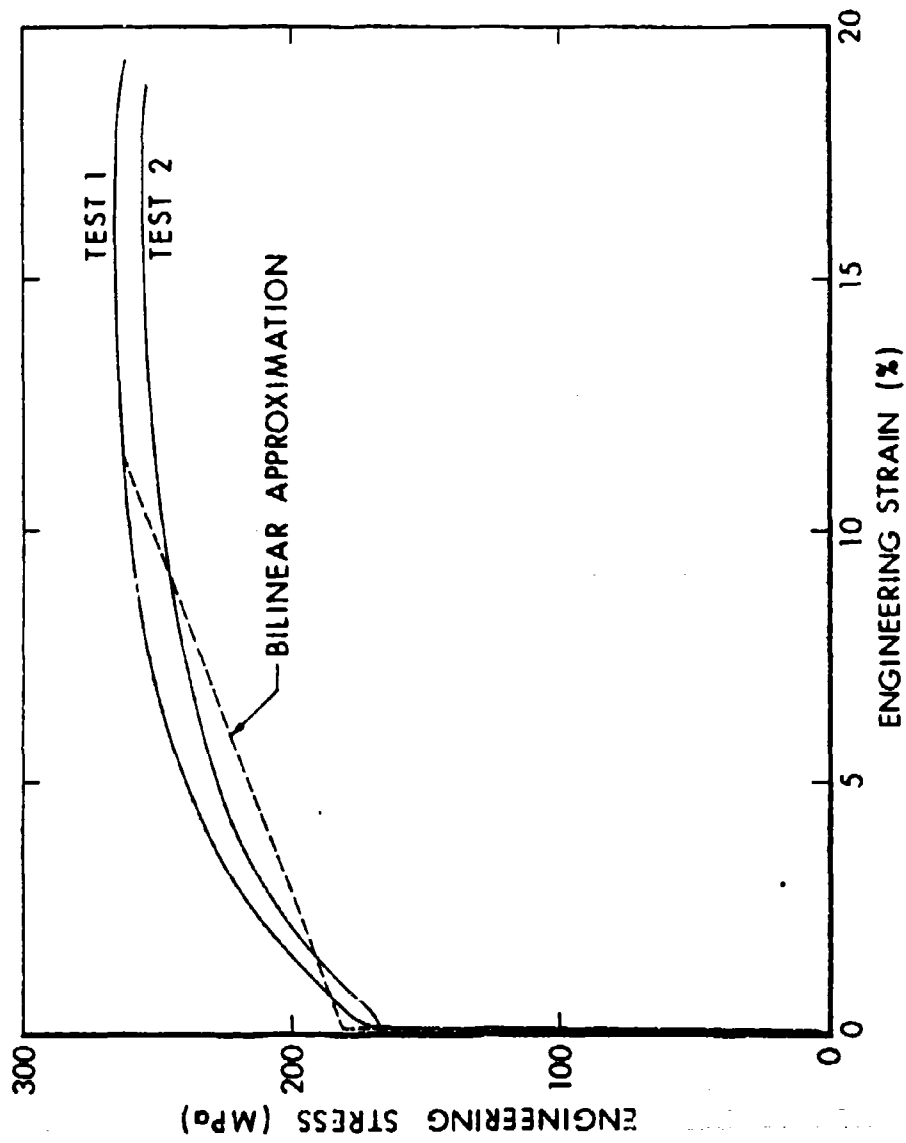


Figure 4. Stress-Strain Curves for the Top Cover Plate Specimens from the TM-46 Mine

Bilinear approximations to the stress-strain curves obtained by averaging the data for the individual specimens are shown superimposed in Figure 4. The ADINA (4, 5) finite element code used in this analysis has a bilinear, elastic-plastic, von Mises yield condition, kinematic hardening, axisymmetric 2-D element for the steel jacket.

The criterion selected to predict failure of the steel casing material was described in Reference 3 as the value of the second invariant of plastic deviatoric strain at failure, I_{2f}^P , defined as

$$I_{2f}(\epsilon^P) = \frac{1}{2} \epsilon_{ij}^P \epsilon_{ij}^P \quad (2)$$

where ϵ_{ij}^P are the plastic component of strains at failure. In the uniaxial tension test where the load is applied in the axial Z-direction we have,

$$I_{2f}(\epsilon_{1-D}^P) = 3/4 (\epsilon_{zz}^P)^2 \quad (3)$$

B. Characterization of Explosive Fills. There are two types of explosive filler materials employed in the TM-46 mine, i.e., TNT as the main charge and tetryl as the fuzewell booster charge.

After surveying the available material properties of explosives and the various 2-D axisymmetric materials models in the ADINA code, the curve description material model (Section XII, pp 17-22, Reference 4) was found to be the appropriate model to use. This model requires tables of loading and unloading bulk moduli and shear moduli versus volumetric strain.

A relationship between the volumetric strain and the bulk modulus obtained from the Mie-Grüneisen equation of state (Reference 1, 6) for shock propagation in solids is given as

$$P(\nu, E) = A\nu + B\nu^2 + C\nu^3 + \Gamma E/\nu \quad (4)$$

where A, B, and C are material constants determined experimentally from Hugoniot-pressure volume states obtained in shock transitions. The above equation characterizes the P, V, and E state variables which are attainable by the solid. In this case the solid is either TNT or tetryl explosive.

The adiabatic loading bulk modulus is defined by

$$\kappa_s = -v \left(\frac{\partial P}{\partial v} \right)_s \quad (5)$$

Assuming that the state of the system is defined by the variables s, E, and V, we have corresponding to the expressions $P = P(V, E)$ and $E = E(V, s)$, respectively,

$$dP = \left(\frac{\partial P}{\partial V}\right)_E dV + \left(\frac{\partial P}{\partial E}\right)_V dE \quad (6)$$

$$dE = \left(\frac{\partial E}{\partial V}\right)_S dV + \left(\frac{\partial E}{\partial S}\right)_V ds \quad (7)$$

Substituting dE from (7) into (6), we find

$$dP = \left[\left(\frac{\partial P}{\partial V}\right)_E + \left(\frac{\partial P}{\partial E}\right)_V \left(\frac{\partial E}{\partial V}\right)_S \right] dV + \left(\frac{\partial P}{\partial E}\right)_V \left(\frac{\partial E}{\partial S}\right)_S ds \quad (8)$$

But from $P = P(V, S)$ we know that

$$dP = \left(\frac{\partial P}{\partial V}\right)_S dV + \left(\frac{\partial P}{\partial S}\right)_V ds \quad (9)$$

Comparing Equations (8) and (9), we have the following expression,

$$\left(\frac{\partial P}{\partial V}\right)_S = \left(\frac{\partial P}{\partial V}\right)_E + \left(\frac{\partial P}{\partial E}\right)_V \left(\frac{\partial E}{\partial V}\right)_S \quad (10)$$

Defining the pressure by the relation

$$P = - \left(\frac{\partial E}{\partial V}\right)_S \quad (11)$$

and substituting this in Equation (9), we have

$$\left(\frac{\partial P}{\partial V}\right)_S = \left(\frac{\partial P}{\partial V}\right)_E - P \left(\frac{\partial P}{\partial E}\right)_V \quad (12)$$

Performing the required differentiation of (4), and using,

$$\left(\frac{\partial P}{\partial V}\right)_E = \left(\frac{\partial P}{\partial \mu}\right)_E \frac{d\mu}{dV} \quad (13)$$

we obtain, after some manipulation

$$\kappa_L = P\Gamma + \Gamma E/V + (1 + \nu)(A + 2B\nu + 3C\nu^2) \quad * \quad (14)$$

Using $P = P(E, V)$ from (4) the relationship between bulk modulus and volumetric strain is given as

$$\kappa_L = \Gamma(\Gamma + 1) E\rho + A + A'\nu + B'\nu^2 + C'\nu^3 \quad (15)$$

*We define volumetric strain ratio, $\nu = (V_0 - V)/V$ and $V_0 = 1/\rho_0$.

where

$$A' = A(\Gamma + 1) + 2B$$

$$B' = B(\Gamma + 2) + 3C$$

$$C' = C(\Gamma + 3)$$

In order to transform Equation (15) to a form $\kappa = \kappa(V)$ the assumptions of unidimensional shock equations and conservation laws of mass, momentum and energy are invoked. The three conservation equations in a frame moving at the shock velocity, U_s , are:

$$\rho V = \rho_0 V_0 \quad (16)$$

$$P + \rho V^2 = P_0 + \rho_0 V_0^2 \quad (17)$$

$$\rho V E + \frac{1}{2}(\rho V)V^2 + PV = \rho_0 V_0 E_0 + \frac{1}{2}(\rho_0 V_0)V_0^2 + P_0 V_0 \quad (18)$$

where V and U are particles velocities, E is the specific internal energy and the quantities with zero subscript are undisturbed values while the quantities without subscripts are applicable behind the shock. In a stationary frame assuming $U_0 = 0$, the following relations between frames of references could be used

$$V = U - U_s \quad \text{and} \quad V_0 = -U_s \quad (19)$$

Substituting above in (16), (17) and (18) the corresponding stationary conservation equations reduce to

$$\rho_0 U_s = \rho(U_s - U) \quad (20)$$

$$P - P_0 = \rho_0 U_s U \quad (21)$$

$$E - E_0 = \frac{(P + P_0)(\rho - \rho_0)}{2\rho\rho_0} = \frac{1}{2}(P + P_0)(V_0 - V) \quad (22)$$

Assuming $P_0 = E_0 = 0$, and substituting E from above into (4), we obtain:

$$P = (A_\mu + B_\mu^2 + C_\mu^3)/(1 - \mu\Gamma/2) \quad (23)$$

Similarly, substituting E from (22) into (15):

$$\kappa_\lambda = \rho P \Gamma (\Gamma + 1) (V_0 - V)/2 + A + A'_\mu + B'_\mu^2 + C'_\mu^3 \quad (24)$$

Finally, substituting P from (23) into (24) the final form is obtained as

$$\kappa_L = \frac{\Gamma(\Gamma + 1)(A\mu^2 + B\mu^3 + C\mu^4)}{2 - \mu\Gamma} + A + A'\mu + B'\mu^2 + C'\mu^3 \quad (25)$$

where

κ_L = the loading bulk modulus

Γ = the Grüneisen coefficient

$A' = A(\Gamma + 1) + 2B$

$B' = B(\Gamma + 2) + 3C$

$C' = C(\Gamma + 3)$

$\mu = \epsilon_V / (1 - \epsilon_V)$

$\epsilon_V = (V_0 - V) / V_0$, volume strain taken positive in compression

$V_0 = 1/\rho_0$ = specific volume at normal conditions.

For the particular case when $\epsilon_V = 0$ which implies $\mu = 0$ and $V = V_0$ it can be easily seen from Equation (25) that $\kappa_0 = A$. Also in the Grüneisen equation of state, at $\epsilon_V = 0$, we take both the pressure and internal energy to be zero. The values for the material constants of the explosives used are shown in Table 1.

TABLE 1. MATERIAL CONSTANTS FOR EXPLOSIVES AND SOIL

Type	ρ_0 (g/cm ³)	Γ	A (Gpa)	B (Gpa)	C (Gpa)	ν
TNT	1.614	.737	10.367	9.101	138.33	.3
TETRYL	1.70	1.6	10.498	17.8	20.6	.3
WET TUFF	2.0	1.5	21.77	32.5	18.33	—

Since data to relate the unloading bulk modulus to the volumetric strain were unavailable, the bulk moduli for unloading were assumed to be identical to the moduli for loading for all explosives. The loading shear modulus, G_L , was obtained from the loading bulk modulus, κ_L , by use of the relationship,

$$G_L = \frac{3\kappa_L(1 - 2\nu)}{2(1 + \nu)} \quad (26)$$

*Here we define specific volume, $V = 1/\rho$ or $\rho V = 1$.

Figures 5, 6 show the dependence of bulk and shear moduli of the two explosives represented by Equations (25) and (26) on volumetric strain. Table 2 gives the values of the two moduli as they were used in the ADINA program. ADINA uses linear interpolation between discrete points.

The tensile volumetric strain at failure of -0.1 per cent as given in Reference 7 was used in calculations for all explosives in this investigation. The method of application of this failure criterion in the ADINA code is through the technique of superimposing on the load-induced strains, a localized gravitational pressure sufficient to cause a hydrostatic compression equal in magnitude to the tensile failure. When the total strain becomes tensile or negative (as per convention used in the material model in the code), a tension cut-off plane is assumed to form normal to the principal strain direction. The normal and shear stiffnesses across this plane are reduced by a factor determined by an input value. One or two additional planes orthogonal to existing cut-off plane (s) are allowed to form if the strain criterion is met. The planes become inactive if compression again develops in the normal direction to the planes.

The pseudo-hydrostatic prestrain is applied by positioning the vertical Z-coordinate at an appropriate negative value. The hydrostatic pressure applied at an element integration point is given for an element, j, by

$$P_j = \rho_e g \sum_{i=1}^N h_{ij} Z_{ij} \quad (27)$$

where

g is the acceleration due to gravity.

ρ_e is the density of the overburden.

h_{ij} is the shape function for node i of element j.

Z_{ij} is the vertical coordinate for node i in element j.

N is the total number of nodes in the element.

The depth of the overburden in terms of the system vertical coordinate position can be obtained from the equation,

$$Z_{ave} = \frac{\kappa_0^f v}{g \rho_e} \quad (28)$$

where

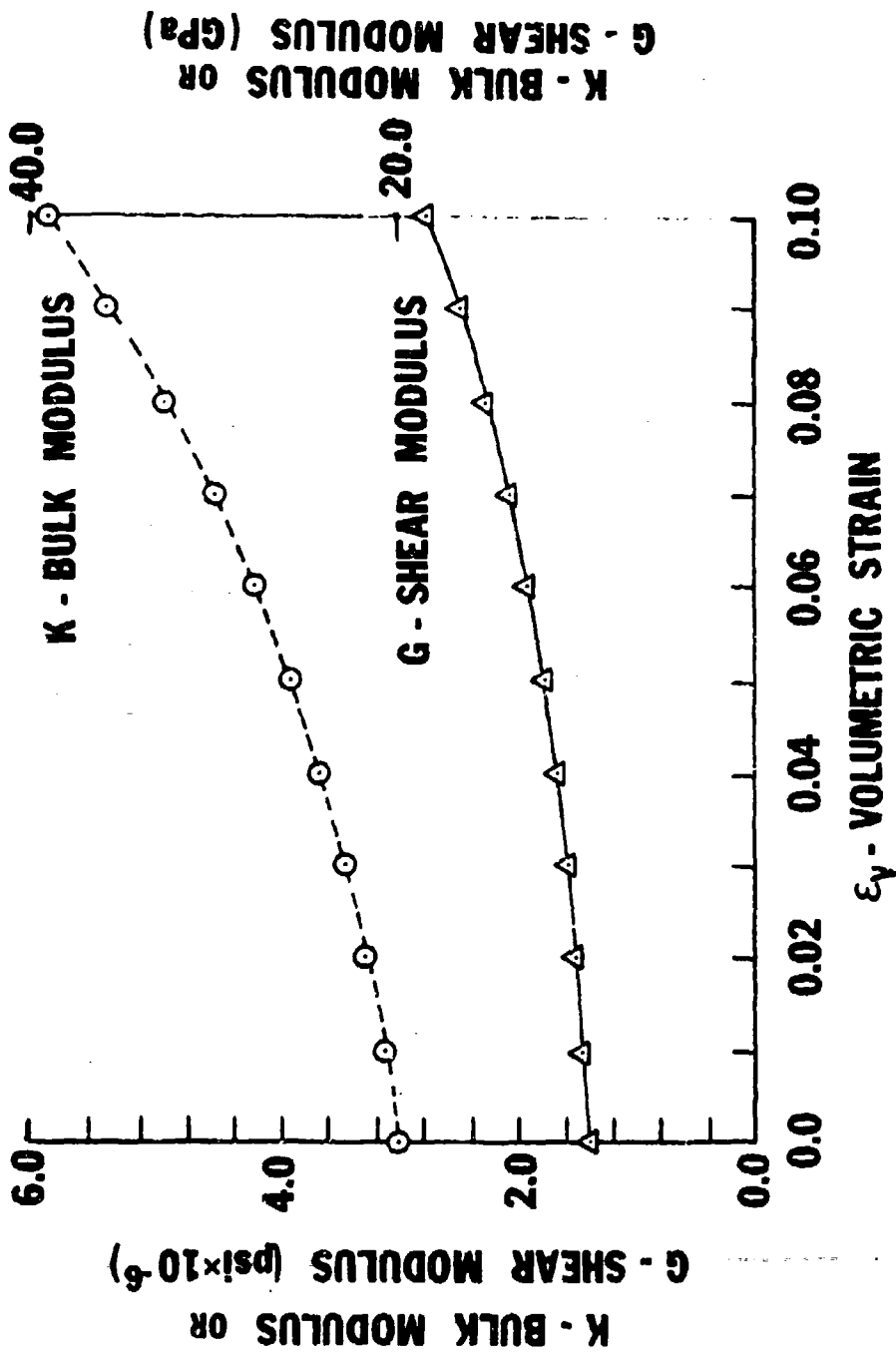


Figure 5. Bulk and Shear Moduli vs Volume Strain for TMT Explosive Used in the TM-46 Mine

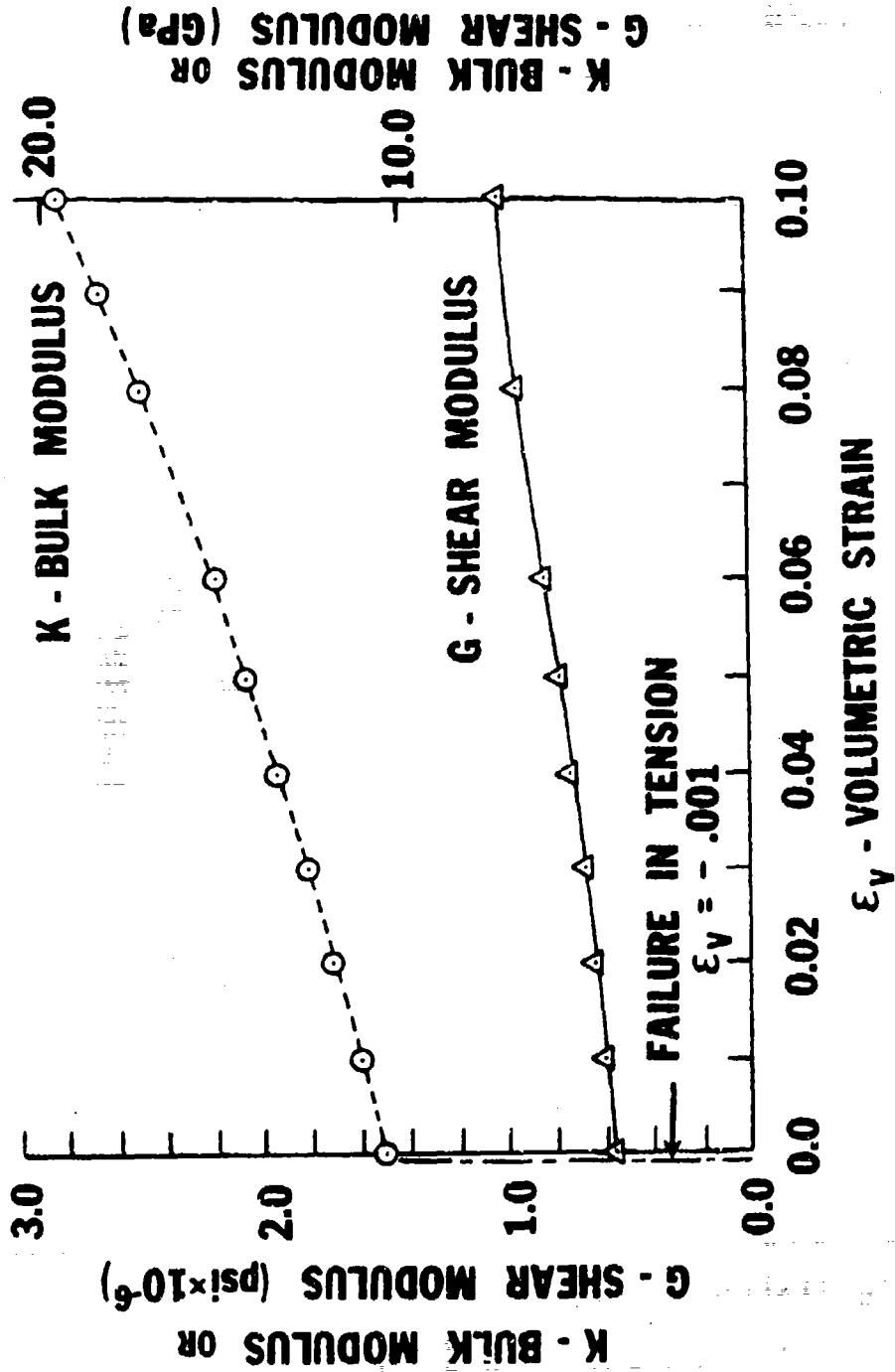


Figure 6. Bulk and Shear Moduli vs Volume Strain for Tetryl Fuze Well Charge of the TM-46 Mine

TABLE 2. ADINA INPUT VALUES FOR BULK AND SHEAR MODULI FOR FILLER MATERIALS

Point No.	<u>TNT EXPLOSIVE</u>			
	ϵ_V (%)	κ_R (GPa)	κ_U (GPa)	G_R (GPa)
1	0	21.72	21.72	10.62
2	1.0	23.03	23.03	11.24
3	3.0	25.65	25.65	12.55
4	5.0	28.68	28.68	14.01
5	9.0	35.85	35.85	17.51
6	11.0	40.20	40.20	19.65
Point No.	<u>TETRYL FILLER</u>			
	ϵ_V (%)	κ_R (GPa)	κ_U (GPa)	G_R (GPa)
1	0	10.5	10.5	4.03
2	1.0	11.15	11.15	4.27
3	3.0	12.59	12.59	4.83
4	5.0	14.24	14.24	5.46
5	8.0	17.2	17.2	6.60
6	10.0	19.56	19.56	7.50
Point No.	<u>WET TUFF</u>			
	ϵ_V (%)	κ_R (GPa)	κ_U (GPa)	G_R (GPa)
1	0	10.37	10.37	4.79
2	1.0	10.78	10.78	4.98
3	3.0	11.93	11.93	5.505
4	6.0	14.62	14.62	6.75
5	8.0	17.24	17.24	7.96
6	10.0	20.64	20.64	9.51

κ_0 is the initial bulk loading modulus,

ϵ_v^f is the volumetric failure strain, negative in tension, and

Z_{ave} is the negative of the distance from the ground surface to the mid-plane of the mine.

C. Soil Simulation. For the structural response calculations of the shallow buried mine, only the top of the mine was exposed to blast pressure while the remainder was assumed to be embedded in soil. In the M-15 mine in Reference 1 an implicit modeling technique was employed whereby nodal tie elements were used to model the base support.

However for the TM-46 mine it is proposed to use an explicit modeling technique whereby initially two compressible layers of soil surrounding the mine body could be included through finite element discretization. Although separation of the mine from the soil medium subsequent to the initial response and sliding phenomenon could not be accounted for, the technique would be a considerable improvement over previous methods due to realistic simulation of the response which includes blast attenuation effects. No simulation of the soil was necessary for the rigid support calculations.

Due to the large variety of soils in which mines would be emplaced, it is possible only to select a soil simulation model which would be representative of some subclass of soils. Thus, a typical shock Hugoniot curve for wet tuff from Reference 8, 9 was selected to define the soil element properties. The data were reduced to a high pressure equation of state and subsequently to a dependent formulation of the bulk moduli on volumetric strain in order to be compatible with the requirements for the tension cut-off curve description model in the ADINA code. For a fully buried mine the soil modeling could be extended in the region above the top of the mine casing and only the top layer of the soil medium could be pressurized by the blast load. The detailed ADINA input values for the soil are shown in Table 2.

D. Simulation of Void in TM-46 Mine. The TM-46 mine has a cavity between the top pressure plate and the middle plate covering the primary charge. This cavity is filled with air which transfers some load to the middle plate as the volume of the cavity is decreased sufficiently. Further uncrimping of the crimped joint connecting the side, top and intermediate walls, due to air compression and angular deflection of the casing near the joint could conceivably occur resulting in loss of some primary explosive charge and consequent deactivation of the mine. Although it is difficult to predict uncrimping using the finite element method, the code could be used profitably to yield moments generated and angular deflection of the casing at critical sections. A separate analysis based on classical theory could then be applied to predict occurrence of uncrimping.

The airgap inside the mine cavity was represented in the finite element model as a set of 2-D axisymmetric fluid elements composed of an inviscid linear compressible material. A constant bulk modulus was used in lieu of a

pressure dependent bulk modulus due to a lack of available data for air. However, the primary difficulty with this model was that there was nothing in the model to prevent the upper plate from penetrating the middle plate as the deformation progressed.

Since the air was judged to apply only a minimal restraint on the motion of the upper plate and due to the need to prevent the two plates passing through one another, a different model has been adopted to simulate contact and avoid interpenetration.

E. Simulation of Contact in TM-46 Mine. Due to lack of contact elements in the code along the interface between the top and intermediate plates substantial interpenetration occurs without any transfer of loading. As a result a major part of deformation is confined to the upper plate, particularly in the stair-cased region, which is clearly unrealistic.

Pending modification of the code to include contact capability, other alternatives were considered to overcome the problem without significantly altering the response behavior in an unrealistic manner. A few alternatives were eliminated due, either to a lack of initial stress input capability, or inability to vary the contact element stiffness as a step function with axial compression at or near the time of contact to prevent overflow at the interface. The model finally selected consists of fictitious axial truss elements connecting the two circular plates. The material model for the trusses is nonlinear and develops only a small force up until the axial strain in trusses approaches -1 . At this strain, a large stiffness is specified to simulate contact between the two plates. Constraints are applied to the upper end of the trusses to insure that its radial coordinate is the same as the radial coordinate at the lower end. Also, the axial coordinate of upper end is constrained to translate with the upper plate. These constraints are necessary to prevent element rotation. The model allows movement only in the axial direction and relaxation upon initial contact but it excludes sliding surface capability which could conceivably be introduced through transverse or radial trusses but would make the model unnecessarily complicated. However, for initial simulation only areas with high probability of contact have been considered for contact simulation.

4. FINITE ELEMENT MODEL DESCRIPTION AND CALCULATIONS.

A. Mesh Generation. The finite element mesh for the mine was generated with the aid of the GEN3D mesh generator program. The mine was modeled as an assembly of axisymmetric 2-D structures using the ADINA finite element code. A six node QUAD element with quadratic displacement interpolation functions in the direction parallel to the surface was used for the steel casing. This type of element models the bending of the thin metal casing better than a four node QUAD. The explosive components were modeled with four-node QUAD elements except where they interfaced the steel jacket, in which case a mid-side node was included on the interface edge. 2×2 Gaussian integration points were used at each element for computational purpose. A total of 304 nodes and 157 elements were used to represent the axisymmetric model.

In ADINA, each material having a distinct material formulation must be modeled as a separate element group. In general four major groups of elements were represented: (1) nonlinear 2-D elements for the steel case, (2) nonlinear curve description 2-D elements for the primary charge, (3) nonlinear 2-D elements for the fuzewell booster charge, and (4) nonlinear truss elements. For the steel case, four material subtypes were used to model the steel properties in different regions of the inhomogeneous mine body. The material model for the casing was a bilinear, von Mises yield condition, kinematic hardening, 2-D axisymmetric element model.

B. Time Step Solution. In ADINA, one has the choice of marching the dynamic solution forward in time via explicit or implicit finite-difference techniques. The implicit schemes are unconditionally stable and can tolerate larger time step size resulting in reduction of computational times. However, equilibrium iteration and stiffness reformation at regular intervals are necessary to obtain meaningful results. In general, it is difficult to make absolute statements as to which is best for a given application. For highly transient shock loads such as shown in Figure 2, it has been our experience that the explicit method gives the higher quality solution for a given amount of central processor computer time. The subject problem was run for a relatively large number of cycles using both explicit and implicit (with equilibrium iterations included) time integration solutions. After a selected amount of problem solution time, the results were compared for solution quality. The explicit solution appeared to have a smoother variation in both displacements and stresses. For this reason, we selected the explicit solution method.

The time step used for the calculations was determined from the Courant stability condition

$$\Delta t = \frac{\Delta t_{crit}}{n} = \frac{\Delta L_{min}}{n \sqrt{E_{y_{max}}/\rho}}$$

where

Δt_{crit} is the minimum Courant stability step size.

ΔL_{min} is the distance between the two closest nodes in the system.

$E_{y_{max}}$ is the Young's modulus for the stiffest material.

ρ is the density of the material,

and n is the number of time steps which we wish to represent the shock wave in passing through the distance ΔL .

The value of Δt_{crit} was approximately 200 nanoseconds and a value of n of four was used, so that the time step for the central difference explicit time integration method was 50 nanoseconds.

C. TM-46 Mine Calculations. The ADINA calculations for the TM-46 mine are in progress. However, some of the salient features of the model have been developed from progress made in studies of the mine thus far. A drawing of the current mesh configuration is shown in Figure 7.

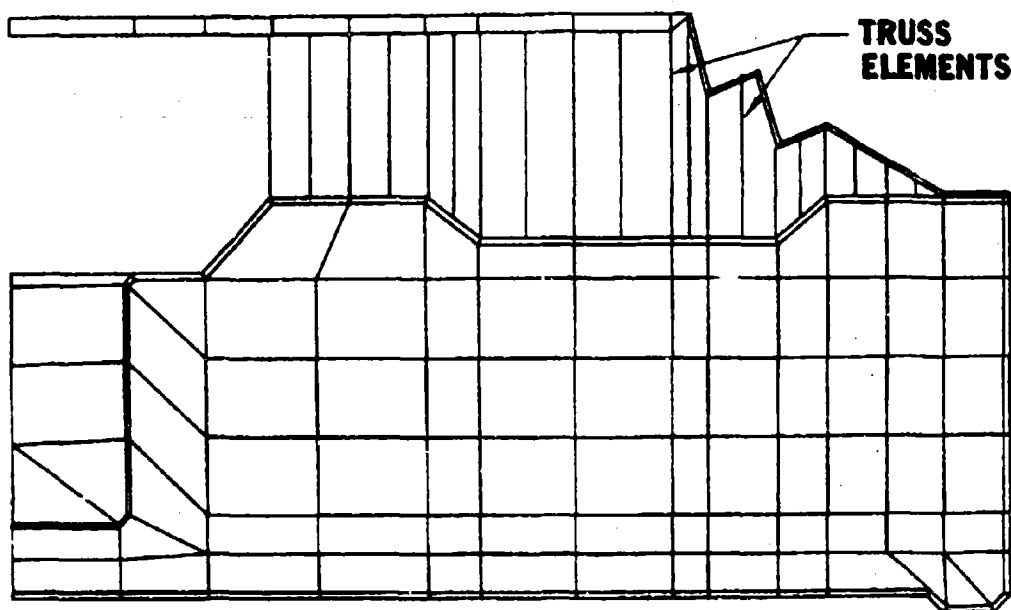


Figure 7. Finite Element Mesh for the TM-46 Mine

Since experimental data indicated significantly varying material properties in different regions of the outer steel jacket of the TM-46 mine several different sets of materials properties were used to model the various steel components of the mine.

At the outset two particular difficulties were expected to be encountered in modeling the TM-46 mine. First, the difference in stiffness between the steel plates and the air filled region leads to numerical problems. The collapse of the air filled region leads to the impact of the upper plate on the middle plate. This phenomenon needs to be modeled rather carefully. Secondly, the thin stepped region of the top cover shown in the upper right part of Figure 7 leads to a very inefficient mechanism for load transfer from the top cover to the main mine body. On the other hand, failure of the top cover may not indicate deactivation of the mine and a viable failure mechanism must inevitably involve a failure of the main mine body.

Since the ADINA code does not currently have a contact element to sense when the top cover plate impacts the intermediate plate, an approach described in Section 3E involving nonlinear truss elements has been used to approximate the interaction of the two plates.

Eigenfrequencies and mode shapes were also obtained for the TM-46 mine in order to ascertain if the model has been formulated correctly and also as an aid in estimating an appropriate time step for the explicit integration scheme. The eigenfrequencies and associated periods for the lower modes are given in Table 3.

TABLE 3. EIGENFREQUENCIES AND PERIODS FOR THE TM-46 MINE

Frequency (cps)	Period (sec)
3041	3.288×10^{-4}
10466	9.555×10^{-5}
17068	5.859×10^{-5}
31071	3.218×10^{-5}

All calculations described herein used the total Lagrangian formulation with a lumped mass matrix with the exception of the nodal tie and truss elements. The formulations used for these were material nonlinearity only and updated Lagrangian analysis procedure, respectively.

5. DYNAMIC RESPONSE PREDICTIONS. Several modifications to the ADINA program were made to assist us in interpreting the response predictions. These are described fully in Reference 1. Due to the very large amount of data available from the ADINA results, search routines were incorporated to identify the extreme (maximum/minimum) stresses and strains in the steel components. Additionally for stresses in the plastic regime a quadratic correction was applied to bring the stress tensor back to the von Mises yield surface and allow calculations to proceed without premature interruptions. The details of these modifications are also described in Reference 10.

From the complex structural construction of the mine, particularly near the stair-cased region in the top plate which appeared to be susceptible to blast induced damage and failure, it was decided to model this region very accurately using shadowgraph measurements. The elements and nodes in the top plate were configured to line up in the axial direction with those in the intermediate plate to facilitate inclusion of contact elements and minimize element rotation.

The initial calculations for the mine on a rigid base support were run without the contact elements to approximately 4000 cycles corresponding to an elapsed time of 0.2 milliseconds. The purpose of the initial runs were to determine the regions and the time of initial contact between the two plates. The results indicated occurrence of initial contact at .06 milliseconds near the crimped region of the mine body and the stair cased region of the top cover.

Failures were predicted in several elements in the stepped regions accompanied by considerable plastic flow. Stresses were significantly high particularly near sharp corners due to acute stress concentration effects. A major part of the response was evident in the top plate while the rest of the mine body did not exhibit any appreciable deformation. The deformation of the mine confined mainly in the area of the top cover plate may not be very realistic since the mine supported on a rigid roller base has unrestrained sidewalls where appreciable deformation is expected but unrealized due to inefficient load transfer mechanism between the top and intermediate walls. One of the chief difficulties encountered has been in trying to provide the appropriate model for the interaction of the top cover plate on the middle plate. We have used the improvisation of nonlinear truss elements (see Figure 7) to simulate the impact of these two components. Since a sudden stiffening of the trusses near the time of contact generated spurious transients and was insufficient to arrest penetration of the intermediate plate due to inertia effects, earlier stiffening of the trusses in a gradual manner initially and at an accelerated rate subsequently as shown in Figure 8 was resorted to. The trusses developed significantly high stresses and internal forces in the region where contact first occurred. Subsequently upon impact the separation of plates caused the stresses in the affected trusses to be released while the next set of trusses in the neighboring region approached impact conditions and developed high stresses which were then released as plates separated and the traveling wave propagated radially inward until the initial contact process was completed. Although the response of the trusses appeared to be realistic, some overflow occurred in the corner region and further stiffening was deemed to be necessary to prevent interpenetration and obtain meaningful results.

A typical response of the system at an early time is shown in Figure 9. In this figure the dotted lines represent the undeformed or original configuration before imposition of the blast load. The vertical lines between the top cover plate and the middle plate represent the nonlinear truss elements. Currently, the calculation has not proceeded to the point where any failure of the main mine body can occur. However, failure of some casing elements in the stepped region has been observed at several time periods beginning at .02 ms and continuing beyond .1 ms when formation of a zone of rupture was indicated in the top cover. However, the main mine body did not show any evidence of failure due to the inefficient load transfer mechanism between the top and intermediate plates. The model of this mine is still evolving and is undergoing modifications to improve accuracy and reliability of prediction.

6. CONCLUSIONS. The soviet TM-46 mine because of its complex stair-cased, double-walled construction was somewhat difficult to model accurately, to analyse and to deactivate. Failure of a particular region of the mine casing itself might not be sufficient to indicate overall failure of the mine. A conservative approach was therefore taken to model the mine by eliminating nonessential details and by requiring defeat of the main mine body through case rupture.

The explicit time integration method appeared to be advantageous for the shock loaded mines due to smoothness of stresses and strains as a function of time. However, second order corrections were necessary to assure that the stress state remained on the yield surface during plastic flow.

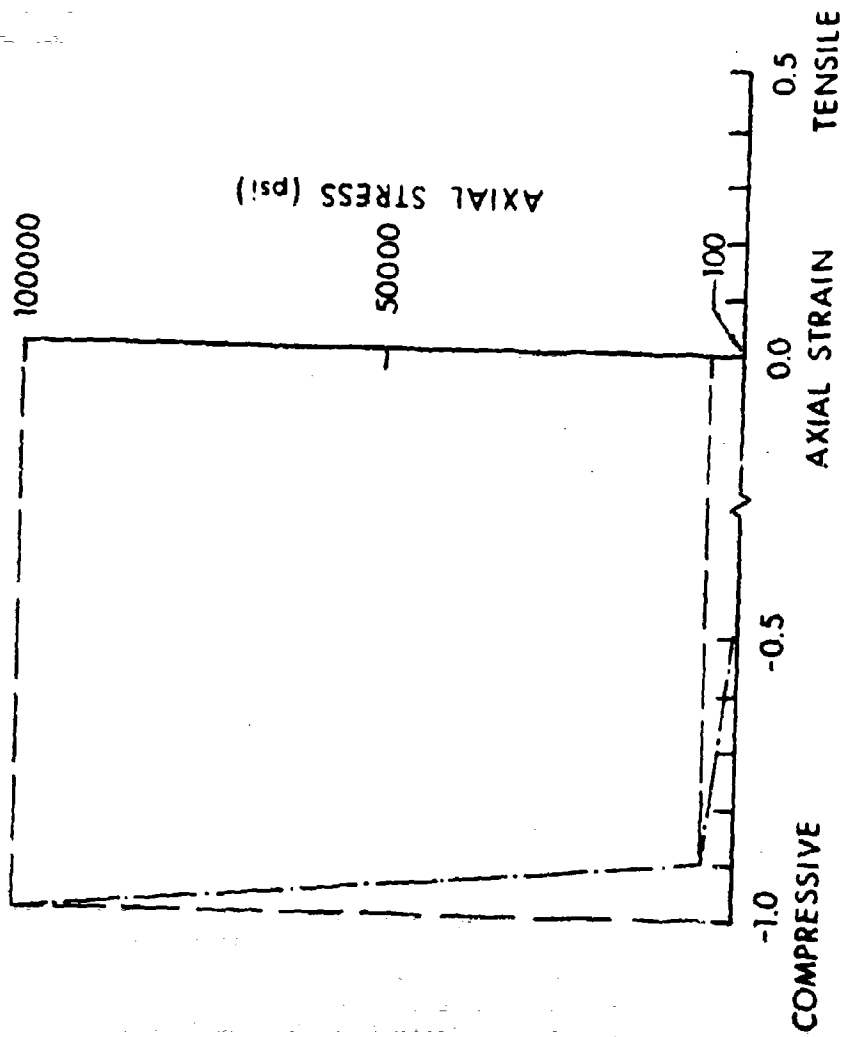


Figure 8. Input Values for Stiffness Variation of Truss Elements Used in the ADINA Code

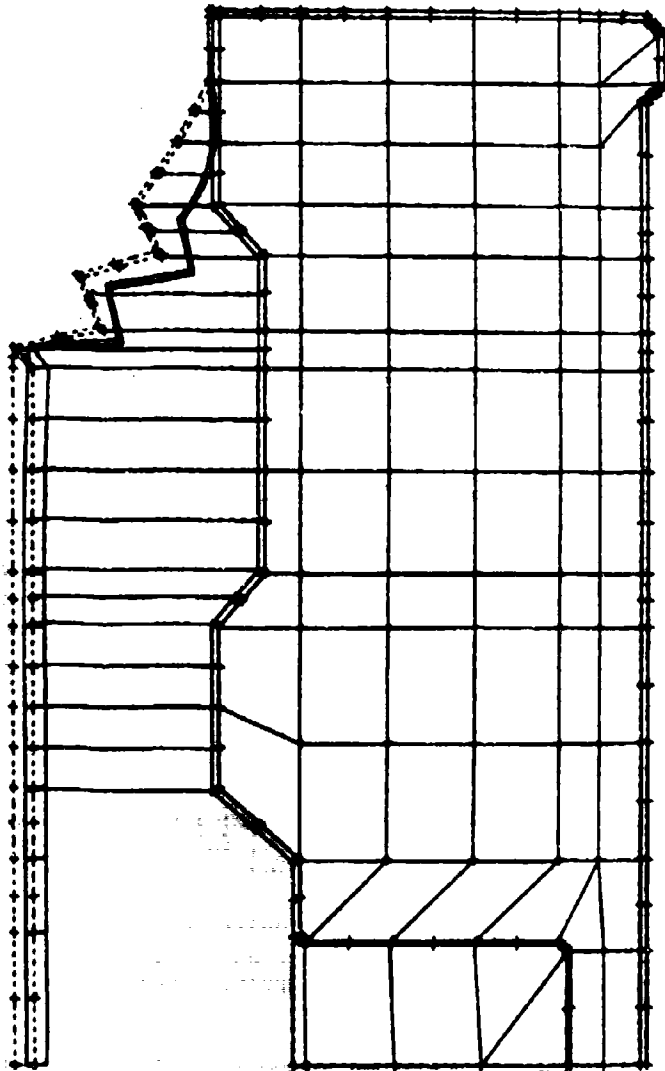


Figure 9. Deformed Shape of the TM-46 Mine on Rigid Support at 75 Microseconds

The parts of the outer steel jacket of the TM-46 mine which are work hardened in the deep drawing metal forming operation have significantly varying materials properties. These variations in stress-strain relations must be measured and modeled carefully since they directly affect mine failure under blast loads.

The contact problem arising from interpenetration of plates results in inefficient load transfer mechanism between the cover and the intermediate plate. Truss contact elements may be used profitably to overcome this shortcoming provided nodal constraints are used to avoid truss rotations.

Linear fluid elements can be used successfully to represent interaction of air in voids with structural response. However, in TM-46 mine it's effect on frequencies and mode shapes is very minimal.

The initial deformation of the TM-46 mine was limited to the response of the top cover plate. The finite element modeling with the ADINA program has presented some difficulty in describing accurately the impact of the top plate on the intermediate plate which contains the primary TNT charge. From past experience main body failure is expected to occur at later times near the corners of the fuze well due to a change of thickness and a sharp radius resulting in significantly high stress concentration and case rupture. This study is still in progress.

ACKNOWLEDGEMENTS. This investigation was a part of a project on mine neutralization research sponsored by the Countermine Laboratory, MERADCOM, Fort Belvoir, VA. Valuable assistance of Messrs Frederick H. Gregory, Charles N. Kingery, Dr. Joseph M. Santiago (BRL) and Dr. John Crawford (Aerospace Corporation) is gratefully acknowledged. Finally, I wish to thank Messrs Robert Franz and Dominic Diberardo for their expert work in measuring the stress-strain properties of the TM-46 mine casing.

REFERENCES.

1. Frederick H. Gregory, "Failure of the M-15 Antitank Mine Due to Blast Loads", BRL Report No. ARBRL-TR-02420, Sep. 1982.
2. Allen J. Tulis et al (IIT Research Institute) and David C. Heberlein et al (MERADCOM), "Improved Fuel Air Explosives", (U) U.S. Army Mobility and Equipment R&D Command Report 2222, Sep. 1977 (S).
3. Frederick H. Gregory, "Finite Element Modeling of the Vulnerability of an M-15 Land Mine Using an Explicit Integration Scheme", Proceedings of the 1981 Army Numerical Analysis and Computers Conference, ARO Report 81-3, Aug. 1981
4. "ADINA, A Finite Element Program for Automatic Dynamic Incremental Nonlinear Analysis", ADINA Engineering, Inc., Watertown, MA, Report AE 81-1, Sep. 1981.
5. K. J. Bathe, "Static and Dynamic Geometric and Material Nonlinear Analysis Using ADINA", MIT-82448-2, May 1977.

6. Brigitta M. Dobratz, "Properties of Chemical Explosives and Explosive Simulants", UCRL-51319 (Rev 1), July 1974.
7. M. S. Chawla and R. B. Frey, "A Numerical Study of Projectile Impact on Explosives", BRL-MR-2741, Apr. 1977.
8. W. E. Johnson and L. R. Hill, "Energy Partitioning During Hypervelocity Impact on Rocks", Rep. No. SC-R-70-4402, Sandia Laboratories, Albuquerque, New Mexico, Dec. 1970.
9. C. A. Hogentogler, Engineering Properties of Soil, First Edition, McGraw-Hill Book Co., 1937, p. 223.
10. Joseph M. Santiago, "On the Accuracy of Flow Rule Approximations Used in Structural and Solid Response Computer Programs", Proceedings of the 1981 Army Numerical Analysis and Computers Conference, Huntsville, Alabama, 26-27 Feb. 1981.

